


Article

Microbial Induced Carbonate Precipitation Using a Native Inland Bacterium for Beach Sand Stabilization in Nearshore Areas

Pahala Ge Nishadi Nayanthara ^{1,*} , Anjula Buddhika Nayomi Dassanayake ²,
Kazunori Nakashima ³ and Satoru Kawasaki ³

¹ Graduate School of Engineering, Hokkaido University, Kita 13, Nishi 8, Kita-Ku, Sapporo, Hokkaido 060-8628, Japan

² Faculty of Engineering, University of Moratuwa, Moratuwa 10400, Sri Lanka

³ Faculty of Engineering, Hokkaido University, Kita 13, Nishi 8, Kita-Ku, Sapporo, Hokkaido 060-8628, Japan

* Correspondence: nishadi.nayanthara@gmail.com; Tel.: +81-80-2123-1764

Received: 4 July 2019; Accepted: 2 August 2019; Published: 6 August 2019



Featured Application: Coastal erosion is a natural process which poses serious problems to coastal communities worldwide. Hard engineering solutions are the most common defense mechanisms that have been used for a long time; although attention has now been inevitably given towards more ecologically and economically sustainable soft engineering approaches. Through this study, it is intended that a bioengineered solution be proposed against coastal erosion using bacterial biomineralization. However, the results presented in this paper are only from a bottom-line study and much more realistic investigations, including scaling up, should be carried out in the future.

Abstract: Microbial Induced Carbonate Precipitation (MICP) via urea hydrolysis is an emerging sustainable technology that provides solutions for numerous environmental and engineering problems in a vast range of disciplines. Attention has now been given to the implementation of this technique to reinforce loose sand bodies in-situ in nearshore areas and improve their resistance against erosion from wave action without interfering with its hydraulics. A current study has focused on isolating a local ureolytic bacterium and assessed its feasibility for MICP as a preliminary step towards stabilizing loose beach sand in Sri Lanka. The results indicated that a strain belonging to *Sporosarcina* sp. isolated from inland soil demonstrated a satisfactory level of enzymatic activity at 25 °C and moderately alkaline conditions, making it a suitable candidate for target application. Elementary scale sand solidification test results showed that treated sand achieved an approximate strength of 15 MPa as determined by needle penetration device after a period of 14 days under optimum conditions. Further, Scanning Electron Microscopy (SEM) imagery revealed that variables such as grain size distribution, bacteria population, reactant concentrations and presence of other cations like Mg²⁺ has serious implications on the size and morphology of precipitated crystals and thus the homogeneity of the strength improvement.

Keywords: beach sand stabilization; coastal erosion; local ureolytic bacterium; microbial induced carbonate precipitation; crystal morphology; nearshore areas

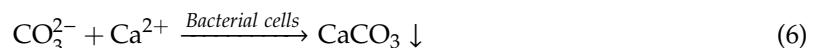
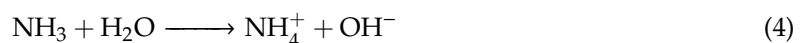
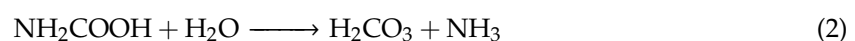
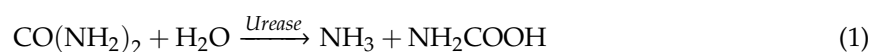
1. Introduction

Microbial Induced Carbonate Precipitation (MICP) through a ureolytic pathway is nowadays a subject of intense research interest in the field of biogeotechnology as it provides solutions to a wider range of engineering applications. Several studies have demonstrated that MICP can be employed to improve the mechanical properties of weak porous materials [1] and cater to a number of

technological applications including ground reinforcement, slope stabilization, liquefaction prevention, erosion prevention of dams and levees, toxic metals removal from contaminated wastewaters/waters, immobilization of hazardous contaminants in soil, and CO₂ sequestration, among others [2–16]. Recently, this mechanism has been suggested as a novel approach towards erosion mitigation of sandy soils in nearshore regions as it is a minimal disturbance to natural coastal environment.

Loose beach sands generally show high erodibility under strong wave action, rising sea levels, as well as under strong wind currents closer to the surface. Conventional engineering solutions such as construction of sea walls, dykes, embankments, groins, and breakwaters have succeeded in combatting the beach sand erosion problem over decades [17,18]. However, they are associated with continual and costly maintenance work, large visual impact lowering the recreational values of beaches and downdrift erosion in the presence of alongshore currents [18]. Chemical grouting is another commonly applied technique in civil engineering to stabilize weaker sands/soils. However, most of the chemical grouts are toxic to humans and require comparatively high cost [1]. Greener solutions such as vegetation belts, sand supply, and artificial dunes are not primary solutions but mere additional measures to protect beaches [17].

The myriad of issues associated with conventional engineering solutions have necessitated a search for alternative measures and, markedly, MICP has gained a lot of attention due to its economical and ecological sustainability. Albeit in limited amounts, previous studies have already shown possible avenues for loose beach sand stabilization for coastal zone management through MICP-based biogeotechnical approaches [19–23]. MICP is based on a set of complex biochemical reactions which ultimately produce calcium carbonate (CaCO₃) crystals that physically bond the loose sand grains together thereby improving mechanical and geotechnical engineering properties of treated sand [24]. In MICP, microbial enzyme urease (urea amidohydrolase; EC 3.5.1.5) catalyzes hydrolysis of urea (CO(NH₂)₂) to ammonia and carbonic acid (H₂CO₃) (Equations (1) and (2)). The resulting ammonia and carbonic acid equilibrate to form HCO₃[−] (Equation (3)) and NH₄⁺ (Equation (4)) with equilibrium constants of pK₁ 6.3 and pK_a 9.3, respectively [25]. This phenomenon creates a high carbonate alkalinity in the micro environment around the cell [26] which favors the formation of carbonate ions (Equation (5)). In the presence or supply of a calcium source, Ca²⁺ ions will be attracted towards negatively charged bacterial cell walls, resulting a localized state of super saturation with respect to calcium carbonate. Subsequently, calcium carbonate will be precipitated on cell surfaces which also act as nucleation sites (Equation (6)) once a certain level of supersaturation is achieved [13].



The enhancement in the mechanical behavior of MICP treated sands is accomplished by a few physical mechanisms based on how calcium carbonate is precipitated with respect to the particles. Calcium carbonate crystals can grow on grain surfaces individually coating them (grain coating), or may precipitate at or near contact points of particles (contact cementing), or grow into the void spaces from particle surfaces, subsequently creating calcium carbonate bridges among sand grains (matrix-supported) [27]. Further, calcium carbonate cements can grow, filling the pore spaces without bridging the sand grains thus lowering the hydraulic conductivity of the treated samples. However,

the overall improvement in the mechanical properties of loose sand following MICP treatment is due to a combination of all four aforementioned cementation mechanisms (Figure 1).

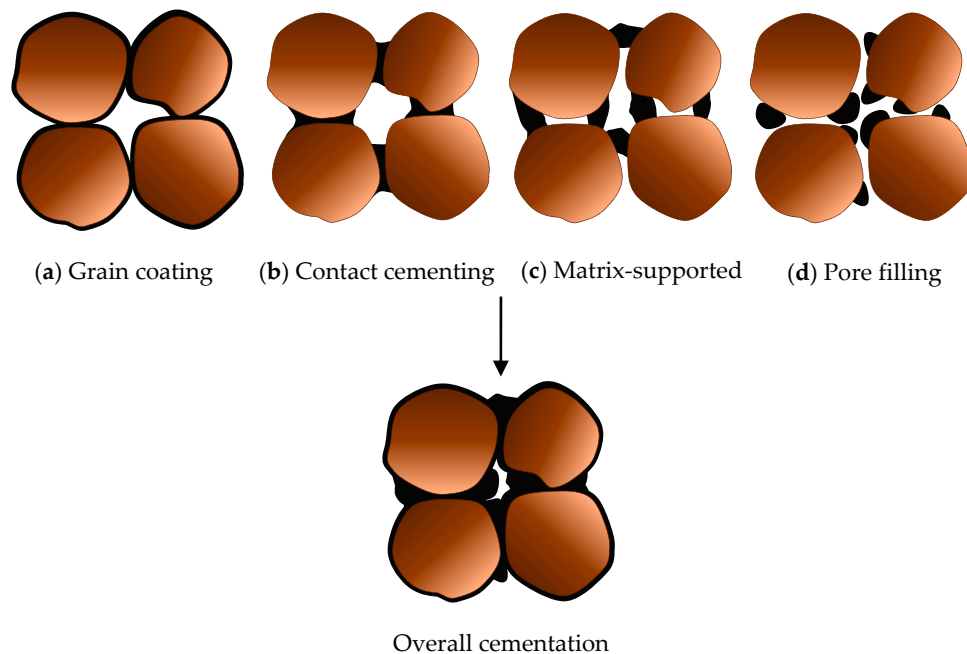


Figure 1. Cementation mechanism of microbial induced carbonate precipitation (a) grain coating; (b) contact cementing; (c) matrix-supported; (d) pore-filling.

Moreover, MICP can be harnessed for in-situ sand/soil applications in two different approaches: biostimulation and bioaugmentation. Biostimulation is the process of modifying prevailing environmental conditions (substrates, nutrients) to encourage calcium carbonate precipitation through enrichment of natural indigenous urea hydrolyzing bacteria [5,28]. Although stimulated ureolytic species are more resilient for in-situ applications, their urea hydrolysis rates seem to be lower than the specialized laboratory cultivated strains [5], and level of MICP will be limited to the initial bacterial cell concentration in the soil [29]. In contrast, bioaugmentation is implemented by supplementing the soil of concern with bacterial strains having specific metabolic capabilities along with nutrient and precipitation media [28,30]. Generally, in-situ bioaugmentation with exogenous strains is challenging as injected foreign cultures may face competition for survival and proliferation among native communities along with poor compatibility in new environments [25,30,31]. Therefore, a more successful approach would be to augment the soil to be treated with native ureolytic bacteria that has been isolated and enriched in laboratory culture media in advance.

The main objective of the present study is to evaluate the effectiveness of MICP treatment via bioaugmentation to stabilize loose beach sand in Sri Lanka, an island highly vulnerable to coastal erosion. As an initial step towards achieving this goal, native ureolytic strains were isolated from Sri Lankan sand/soil and assessed for their potential for bioaugmentation. Upon receiving more successful results for MICP treatment using an inland ureolytic bacterium than that from local marine bacteria for the desired engineering application, further studies were carried out to (i) optimize the growth and enzymatic activity of the isolated strain, (ii) address mechanical behavior and microstructure of the MICP-treated sand and (iii) explore the versatility of the isolated inland strain to perform biomediated calcium carbonate precipitation in nearshore environments as an alternative technique for sand stabilization.

2. Materials and Methods

2.1. Isolation and Identification of a Suitable Urease Active Bacterium

2.1.1. Soil Sampling and Isolation of Ureolytic Bacteria

The coastal hydrodynamics along the southern, south western, and western coastal belt of Sri Lanka are highly affected by the strong waves generated by the south western monsoon and are the most susceptible to erosion of sandy slopes. Therefore, the study area for the current study was demarcated from Tangalle in southern province to Uswetakeiyawa, Colombo, in western province. Beach sand samples, each approximately weighing 50 g, were randomly collected from 11 sampling locations (M1–M11) along the shoreline and soil samples from 2 inland localities (L1 and L2) into sterile tubes (see Supplementary Materials). All the samples were exported from Sri Lanka to Japan following the Japanese Minister Permission System and stored at 4 °C. Each soil sample of 5 g was then serially diluted (10^{-1} – 10^{-6} times) under sterile conditions. 50 µL of beach sand and inland soil suspensions thus prepared were then plated on Zobell 2216E agar medium (5.0 g/L hipolypeptone, 1.0 g/L yeast extract, 0.1 g/L FePO₄, 30.0 g/L agar in artificial seawater, pH 7.6–7.8) and NH₄-YE agar medium (15.75 g/L tris buffer, 10.0 g/L (NH₄)₂SO₄, 20.0 g/L yeast extract, 20.0 g/L agar in distilled water), respectively. After incubating at 30 °C for 2 days, colonies were identified from a plate with 30–200 colonies. Different types of colonies were visually identified and separately cultivated on the plates prepared in the same manner described above.

A simple urease activity test was then conducted for qualitative assessment of urease producing bacteria. Each colony was mixed with 20 mL of cresol red solution containing urea (0.4 g/L cresol red and 25 g/L CO(NH₂)₂ in distilled water) and incubated at 45 °C for two hours. Colonies that changed the initial yellow color to pink (Cresol red changes from yellow to pink when pH changes to 7.2–8.8, which is accomplished during urea hydrolysis) were identified as urease active bacteria.

2.1.2. Identification of Bacteria by 16S rRNA Sequencing

16S rRNA gene amplification and sequencing was carried out for selected ureolytic isolates. The analysis of the DNA sequences was performed by using the DB-BA 12.0 (Techno Suruga Lab Co., Ltd., Shizuoka, Japan) and International Nucleotide Sequence Database (DDBJ/ENA (EMBL)/GenBank) by Techno Suruga Laboratory, Shizuoka, Japan.

2.1.3. Cultivation of Bacteria and Assessing the Potential for Microbial Induced Carbonate Precipitation

Zobell 2216E for marine bacteria and NH₄-YE medium for land bacteria were used for culturing under sterile aerobic conditions. The cells were precultured separately in 5 mL of each media at 30 °C and 160 rpm for 24 h. One mL of the preculture was inoculated with 100 mL of the fresh medium and incubated under the same conditions. Microbial cell growths of the isolates were determined in terms of optical density at a wave length of 600 nm (OD₆₀₀) using a UV–vis spectrophotometer (V-730, JASCO Corporation, Tokyo, Japan) from representative specimens sampled at regular intervals of 24 h.

Microbial induced calcium carbonate precipitation tests were conducted in 10 mL tubes to evaluate feasibility of using isolated bacterial strains for biomediated soil improvement. Calcium chloride (CaCl₂) reagent was chosen as the calcium source and 1 mL from equimolar concentrations (0.5 mol/L (M)) of CaCl₂ and urea solutions were used. One mL from the bacteria culture was added to the tube and total volume was adjusted to 10 mL using distilled water. Samples were then kept in a shaking incubator at 30 °C and 160 rpm for 48 h. Finally, the reaction mixtures were centrifuged and precipitates were collected to gravimetrically compare the amount of precipitate formed by each isolate. Based on the results, a single isolate was picked as the most suitable for further analysis.

2.1.4. Microbial Cell Growth and Urease Activity Measurement

Urease activity of the selected isolate was evaluated by cells suspended in a solution containing urea in terms of the amount of enzyme required to hydrolyze one micromole of urea per minute (U) per milliliter following the method explained by Gowthaman et al. [3]. The test was repeated at 24 h intervals to determine the temporal stability of the urease enzyme for bacteria cultured at different temperatures ranging from 20–50 °C.

In order to monitor the pH dependency of the enzymatic activity, the urease activity test was performed for 1 mL samples collected from a bacterial cell culture incubated at the optimum temperature (decided from the above step) and subsequently suspending them in substrate solutions prepared with different pH values (ranging from pH 5–9).

2.2. Small Scale Sand Solidification Test

Centimeter-scale one-dimensional column specimen tests under different experimental conditions were performed as a preliminary step towards elucidating the potential for strengthening and stabilizing loose beach sand by MICP.

Two types of natural beach sands with varying particle size gradations (see Supplementary Materials) collected from Sri Lanka were used in the current study; a well graded sand and a uniformly graded sand (herein after referred to as sand 1 and sand 2, respectively). The particle size distribution curves were obtained by sieve analysis using BS410 standard sieves. The characteristics and chemical composition of the sands (as determined from powdered samples using Energy Dispersive X-ray Fluorescence spectrometer (JSX-31000R II JEOL, Ltd., Tokyo, Japan) at Material Analysis and Structural Analysis Open Unit of Hokkaido University, Japan) are tabulated in Table 1.

Table 1. Characteristics of natural beach sand used in the current study and their elemental composition.

Sand Type	ρ	D ₅₀	C _u	C _c	Elemental Composition (%)									
					Al ₂ O ₃	SiO ₂	CaO	TiO ₂	Cr ₂ O ₃	Fe ₂ O ₃	NiO	CuO	SrO	PbO
Sand 1	2.81	0.37	3.58	1.12	3.64	75.39	4.25	8.39	0.04	8.13	0.08	0.07	-	-
Sand 2	2.68	0.61	1.51	0.93	-	24.14	71.79	0.27	-	2.98	0.04	-	0.61	0.06

ρ —specific gravity; D₅₀—diameter at which 50% of the sample's mass is comprised of smaller particles than that value; C_u—coefficient of uniformity; C_c—coefficient of curvature.

The optical density (OD₆₀₀) of the harvested culture varied between 2.0 and 2.5 and all the solidification tests were conducted at an optimum temperature of 25 °C for a treatment period of 14 days. 0.5 M and 1.0 M Ca²⁺ cementation solutions prepared with distilled water were used to examine the effect of Ca²⁺ ion concentration on solidification of sand. The 0.5 M cementation solution composed of 30.0 g/L of urea (CO(NH₂)₂), 55.0 g/L of CaCl₂, and 3.0 g/L of nutrient broth.

A standard size 35 mL syringe (2.5 cm diameter) was used for the sand solidification tests. In each case, sand was oven dried at 105 °C for 48 h and a predetermined weight of sand was compacted in 3 layers by applying 20 hammer blows on each layer. The bottom face of each column was blocked by a filter paper.

After considering the studies pertaining to determine the most favorable and proper treatment method for MICP applications, a method involving cycles of batch treatment of bacterial culture and cementation solution was adopted for this study. Firstly, a 12 mL of bacterial culture was injected from the top of the syringe, excess solutions were drained out at a controlled rate and allowed approximately 2 h for bacteria fixation. Secondly, this was followed by 12 mL of cementation solution, supplying the necessary nutrient and precipitation components.

Moreover, in terms of saturation level, the entire length of the sand column was retained under fully saturated condition as an initial test condition. Four test cases were carried out, varying the

reactant concentration and frequency of bacteria injection. For cases 1 and 3, the bacterial culture solution was injected only in the beginning (day 0) whereas for cases 2 and 4, the solution was injected twice, on day 0 and day 7. Cementation solution was injected every 24 h for the total treatment period. However, 0.5 M cementation solution was injected for test cases 1 and 2 while 1.0 M solution was supplied to test cases 3 and 4.

2.3. Effect of Mg^{2+} on Microbial Induced Carbonate Precipitation

The majority of the MICP-based studies carried out so far has assessed the change in soil properties with calcium carbonate precipitation. However, the real field conditions are such that it is likely to contain other impurities and cations that may interact with the precipitation process. For the implementation of MICP for the desired application in nearshore environments, attention has to be paid to the fact that target treatment environments will consist of a considerable amount of magnesium ions. Therefore, a set of experiments were conducted incorporating both Mg^{2+} and Ca^{2+} ions with various Mg^{2+}/Ca^{2+} molar ratios from 0 to 1.

Anhydrous magnesium chloride was used as the Mg^{2+} source. Microbial induced carbonate precipitation tests were carried out as described above, but according to the test program in Table 2. Sand solidification tests were done using “sand 2” under fully saturated conditions for the same Mg^{2+}/Ca^{2+} molar ratios employed in precipitation tests.

Table 2. Microbial induced carbonate precipitation and sand solidification test conditions with magnesium addition.

Test Case	Mg^{2+} (M)	Ca^{2+} (M)	Mg^{2+}/Ca^{2+} Ratio	Sum of Mg^{2+} and Ca^{2+} (M)	Urea (M)
1	0.00	0.50	0.00	0.50	0.50
2	0.10	0.40	0.25	0.50	0.50
3	0.15	0.35	0.43	0.50	0.50
4	0.25	0.25	1.00	0.50	0.50

2.4. Monitoring Methods

2.4.1. Needle Penetration Device

The local cementation strength of the specimens along the height of the column was examined in terms of estimated unconfined compressive strength (UCS) using a soft rock penetrometer (SH-70, Maruto Testing Machine Company, Tokyo, Japan). The needle of the device was penetrated into the sand specimens at three locations (1, 3, and 5 cm from the bottom of the column) and the penetration resistance (N) and penetration distance (mm) were simultaneously measured. From the results, a “penetration gradient” (N/mm) was determined, which was ultimately used to estimate UCS using Equation (7) where x is the penetration gradient and q_u is the UCS.

$$\log(q_u) = 0.978 \log(x) + 2.621 \quad (7)$$

The regression relation in Equation (7) has been developed by analyzing an adequate number of natural soft rock samples and cement based improved soils and confirmed by a correlation coefficient of 0.914.

2.4.2. Scanning Electron Microscopy (SEM) Analyses

Fractions of cemented sand collected from different parts of the oven dried column were observed under a Scanning Electron Microscope (SuperScan SS-550, Shimadzu Corporation, Kyoto, Japan) to study the soil matrix biocemented with calcium carbonate.

2.4.3. X-ray Diffraction (XRD) Analyses

X-ray diffractometer patterns of the powdered precipitates from Section 2.3 were analyzed using an X-ray generator (MiniFlex™, Rigaku Co., Ltd., Tokyo, Japan). The analysis was carried out at room temperature using the XRD machine with CuK α radiation at a rate of 6.5° 2 θ /min and a step size of 0.02° 2 θ ranging from 10 to 80° 2 θ . Qualitative mineralogy of the samples was determined with the standard interpretation procedures of XRD using Match! software for phase identification from powder diffraction.

2.4.4. X-ray Fluorescence (XRF) Analyses

The quantitative elemental analysis of the powdered sand samples was determined using an Energy Dispersive X-ray Fluorescence spectrometer (JSX-31000R II JEOL, Ltd., Tokyo, Japan) at the Material Analysis and Structural Analysis Open Unit of Hokkaido University, Japan. The instrument consisted of a 5–50 kV, 1 mA, 50 W X-ray generator. Samples were observed by a colorful CCD camera.

3. Results and Discussion

3.1. Isolation and Identification of a Suitable Urease Active Bacterium

Although a total of more than 100 bacterial strains were isolated from different soil samples, urease producing bacteria were encountered in only 6 locations. Apparently, the proportion of ureolytic bacteria in each case was smaller than that of non-ureolytic bacteria except for location L2 (Figure 2). As per these results, it is evident that ureolytic bacteria are not ubiquitous in the dynamic coastal regions as much as in the inland environments. Based on the simple urease activity test and the corresponding increase in pH in reaction mixture during first 24 h (data not included), 6 isolates were considered for further analysis. The phylogenetic groupings of the chosen isolates are shown in Table 3.

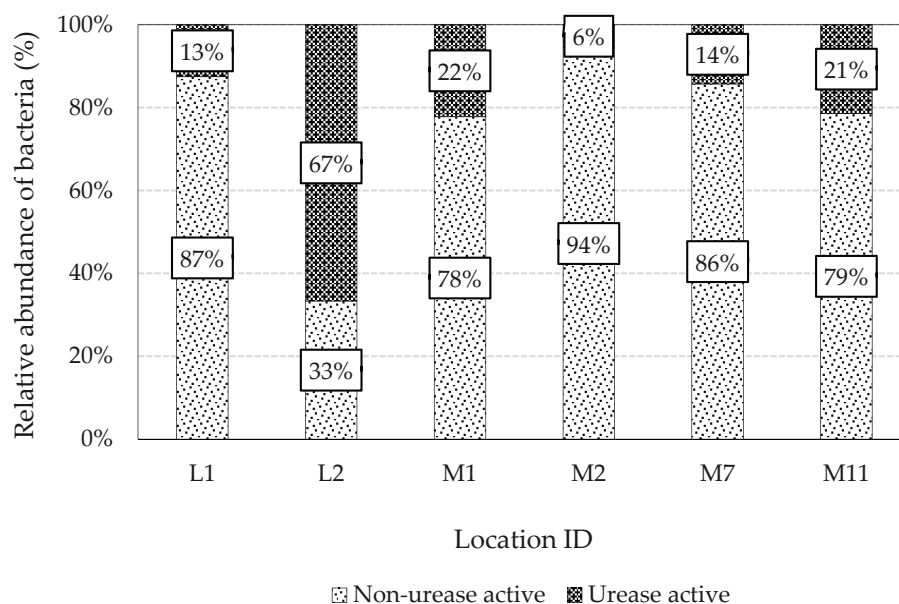


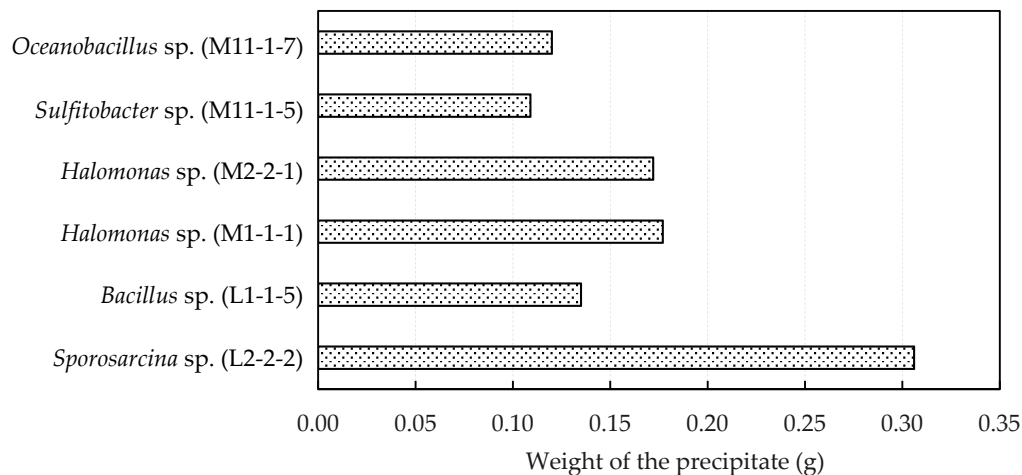
Figure 2. Relative abundance of ureolytic bacteria in different sampling locations.

Table 3. Phylogenetic grouping of the isolated bacterial strains.

Sample ID	Closest Match to Phylogenetic Grouping	Genbank Accession Number	Similarity
M1-1-1	<i>Halomonas</i> sp.	AJ306891	99.8%
M2-2-1	<i>Halomonas</i> sp.	AJ306888	99.6%
M11-1-5	<i>Sulfitobacter</i> sp.	AY180103	98.0%
M11-1-7	<i>Oceanobacillus</i> sp.	HQ595230	99.9%
L2-2-2	<i>Sporosarcina</i> sp.	HQ676600	99.7%
L1-1-5	<i>Bacillus</i> sp.	NR_146034	98.7%

In terms of OD_{600} , all the isolates showed a stable growth at 30 °C. However, the strain belonging to *Sporosarcina* sp. preferably witnessed a more stable growth over the entire test period (see Supplementary Materials).

The test tube precipitation test results are a good relative indication of the potential of each strain for sand solidification by MICP [32] as the strength improvement is proportional to the amount of bio-precipitate formed. The results indicated that the strain belonging to *Sporosarcina* sp. shows the highest performance for microbial induced carbonate precipitation and the weight of precipitate is approximately twice as that from others (Figure 3). The strains belonging to *Sporosarcina* sp. strain are gram stain positive, rod shaped, motile, aerobic nonpathogenic bacterium which produces active intracellular urease in large quantities [13,33–37].

**Figure 3.** Microbial induced carbonate precipitation capacity of isolated strains.

On the other hand, strains belonging to *Sporosarcina* sp., specially *Sporosarcina pasteurii*, has been extensively studied for a vast variety of MICP applications and has shown successful results [13,15,16,33,35,38–42]. More interestingly, this specific strain has the ability to tolerate extreme conditions, for example pH levels as high as 9 [43], making it a good candidate for the target application. Considering all these facts, the *Sporosarcina* sp. strain was identified as the most suitable bacterium, and remaining laboratory investigations were carried out employing this strain.

3.2. Optimizing the Growth and Enzymatic Activity of the Isolated *Sporosarcina* sp. Strain

3.2.1. Effect of Temperature

In order to ascertain the maximum benefits from the MICP process, it is important to determine the temperature at which microbial growth and urease activity is optimum. As per the findings of this

study, the microbial growth of the isolate was more stable and comparatively higher at a temperature range of 20–25 °C whereas the growth became almost zero when the temperature was raised up to 50 °C (Figure 4). Ng et al. [12] states that the microbial growth is generally less sensitive to temperature changes over the range of 20–30 °C, which was also true in this case. In addition, the strain exhibits the typical growth curve of a bacteria population over time where cell growth increases exponentially up to a maximum followed by a stationary phase and then a gradual fall (death phase) due to independent or combined effect of nutrient exhaustion, waste accumulation and/or oxygen depletion, and subsequent cell lysis [44].

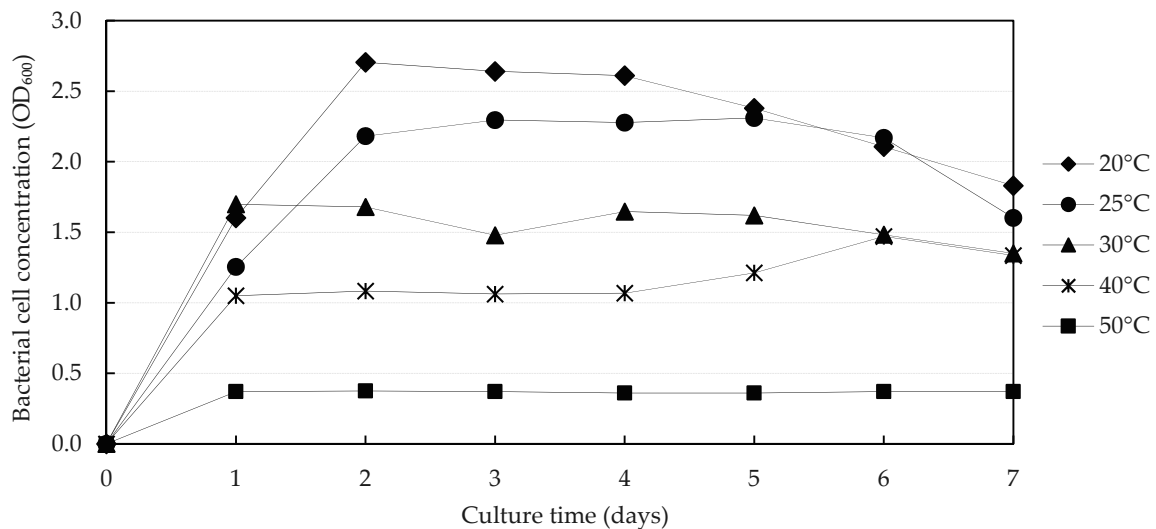


Figure 4. Variation of bacterial cell concentration of *Sporosarcina* sp. at different temperatures.

Catalysis of urea hydrolysis is a temperature dependent enzymatic reaction [43] and is closely associated with the bacterial cell population [12]. The effect of temperature on urease activity of the isolate is presented in Figure 5 indicating that enzymatic performance is maximum and stable at 25 °C. The activity is degraded almost to zero at 40 °C and 50 °C. This is in accordance with the findings of Dhami et al. [45] where microbial enzyme activity of *Bacillus megaterium* decreased by a fraction of 47% when temperature was raised from 35 to 55 °C. In contrast to that, Sahrawat [46] in a very early study revealed that optimum urease activity lies at temperatures close to 60 °C. This was later attested to by Liang et al. [47] and few others for strains *Streptococcus salivarius* [48] and *Parahodobacter* sp. [49]. In terms of temporal stability, although the selected bacterium maintains a relatively satisfactory enzyme stability over a period of 7 days, the activity seems to drop over time as cell lysis and denaturation of the loose enzyme take place [50]. However, considering the above results as well as the tropical climate in Sri Lanka, the remaining investigations were carried out at a temperature of 25 °C.

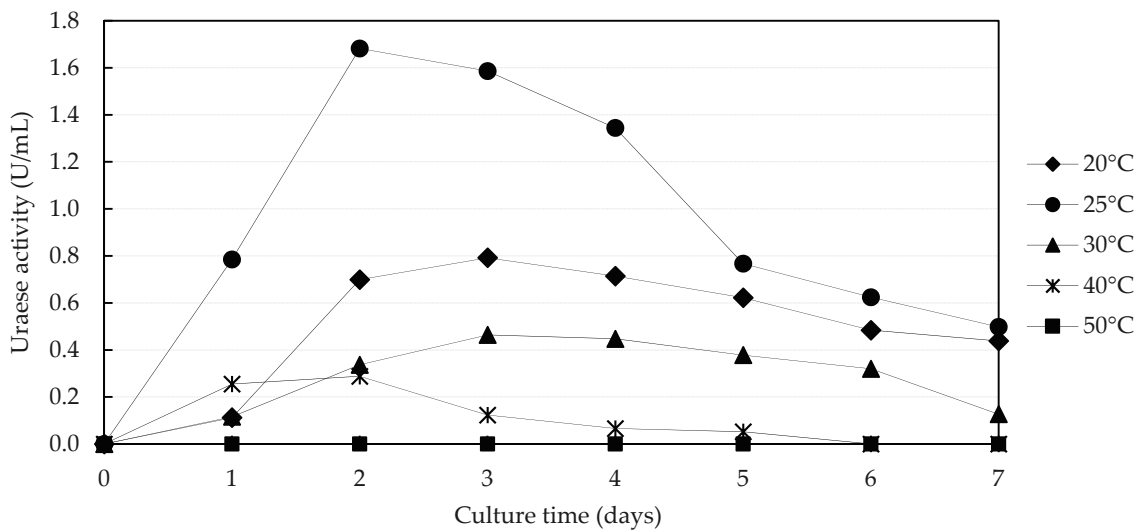


Figure 5. Variation of urease activity of *Sporosarcina* sp. at different temperatures.

3.2.2. Effect of pH

pH has a significant influence on urease activity and, hence, the success of MICP. Under highly acidic or alkaline conditions, the urease enzyme is generally irreversibly denatured [49,51]. Figure 6 depicts the degree of change in urease activity at different pH levels. It is evident from the results that, urease activity increases rapidly from pH 6.0 to 9.0 and the enzyme is comparatively more active in the pH range 7.5–9.0. Mobley et al. [51] reported that majority of the microbial ureases, except for a few acid ureases, are optimum under neutral pH conditions. However, the findings of Stocks-Fischer et al. [13] are on the same trend as this study: They reported that urease activity of *Sporosarcina pasteurii*, drastically increased from pH 6.0 to 8.0 and gradually reduced thereafter. Nevertheless, the activity at pH 9.0 for that specific strain was still satisfactory for MICP applications. Ciurli et al. [52] are other researchers who have shown that optimum pH for urease activity of *S. pasteurii* is 8.0. Moreover, few other microbial strains have showed their optimum performance at pH 8.0, as reported in literature [49,53]. From the aforementioned results, it is clear that the isolate used in this study is moderately alkalo-tolerant and can be successfully employed for the target application in a coastal environment.

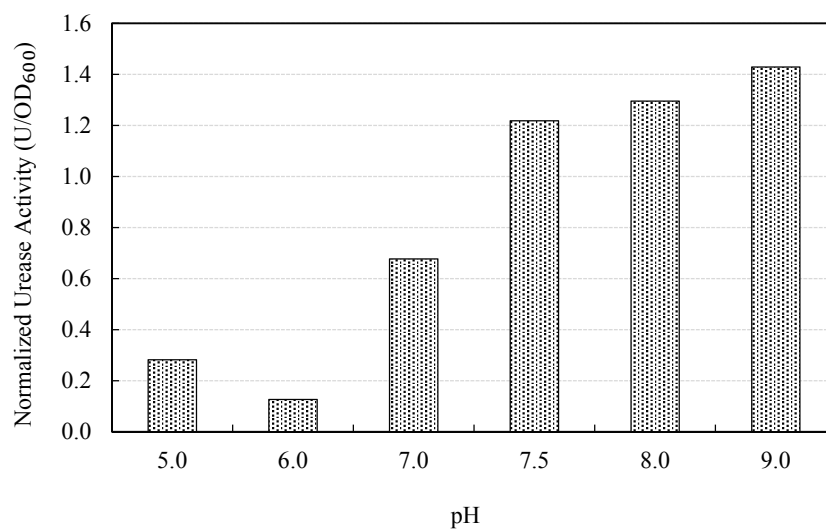


Figure 6. Variation of urease activity of *Sporosarcina* sp. at different pH conditions.

3.3. Potential for Beach Sand Solidification by MICP Treatment

3.3.1. Effect of Bacteria Population and Reactant Concentration

The reactant and the bacteria cell concentration are two primary factors that governs the degree and the homogeneity of the strength increment over the treatment depth. The local strength of sand specimens underwent different treatment conditions with respect to the aforementioned two parameters, are illustrated in Figure 7. However, the cementation reagent contained equimolar concentrations of urea and CaCl_2 as in Ng et al. [54]. All the samples were strongly cemented and the estimated average (as well as individual) UCS values from two independent tests for all the cases were above 3 MPa. When the two samples injected with 0.5 M cementation solution were considered, it was clear that the specimen with bacteria injected twice showed a significant strength increment than that of the specimen injected with bacteria only in the beginning. According to previous records, it is deduced that higher concentrations of bacteria populations enhance the amount of CaCO_3 precipitate and, thus, the results of MICP treatment [41]. Generally, bacteria play two key roles in the biocementation process; (i) catalysis of urea hydrolysis and (ii) provision of nucleation sites [55]. The initial investigations on urease activity of the isolated strain showed that enzymatic activity diminishes over time. Besides, there are several other factors that may gradually inhibit the bacteria's affinity to perform their intended role as a catalyst for urea hydrolysis over the entire treatment time period. Possible reasons are hydraulic constraints such as cell encapsulation from the resulting precipitate or being confined inside pores, restricted movement of nutrients and precipitation components as pore spaces get narrowed after initial precipitation, space constraints in the case of saturated conditions, accumulation of metabolic wastes and also flushing out of bacteria [50,56]. Further, bacterial cell walls act as nucleation sites for CaCO_3 precipitation in biochemical processes [13,57] and some of the above mentioned factors may lower the availability of cells that can serve this purpose. Therefore, it is concluded here that the rate of urea hydrolysis and subsequent biocementation was retarded over time in the case where bacteria was injected only in the beginning, whereas the urease activity was regained and number of nucleation sites were improved with the reinjection in the case where culture was injected twice, leading to a better performance. This phenomenon was further confirmed by the measurement of Ca^{2+} concentration and the pH of the samples collected from the solution draining out from the outlet (Figure 8). Better performance of microbial induced carbonate precipitation was characterized by lower Ca^{2+} concentration and higher pH values as soon as the bacterial culture was injected.

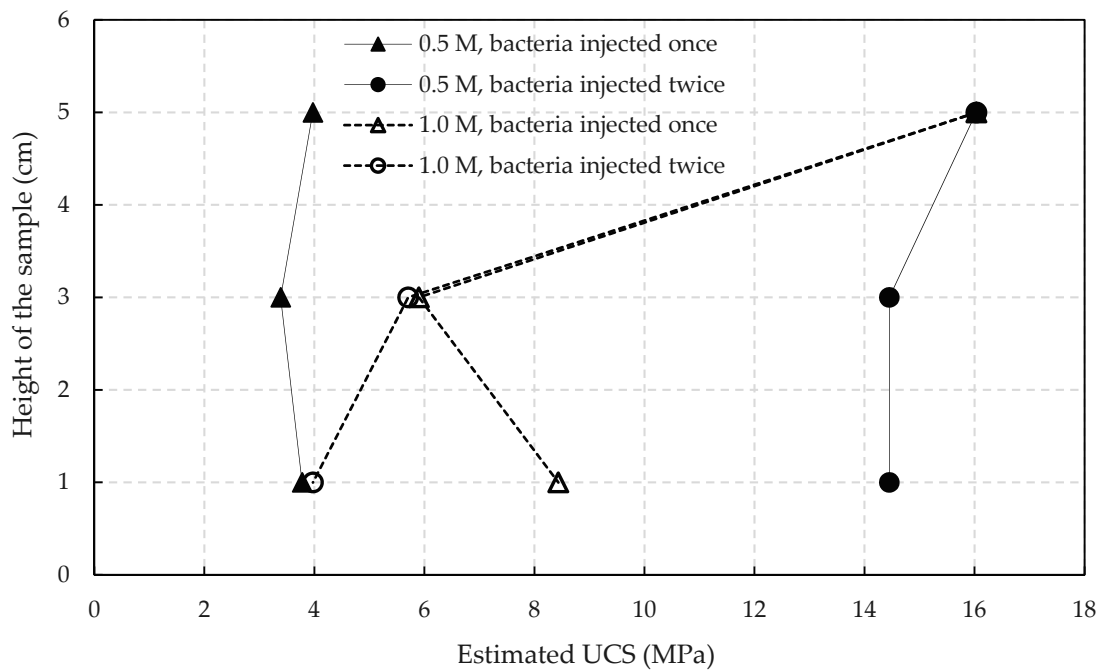


Figure 7. Variation of local strength of microbial induced carbonate precipitation (MICP) treated sand under different bacteria and reactant concentrations.

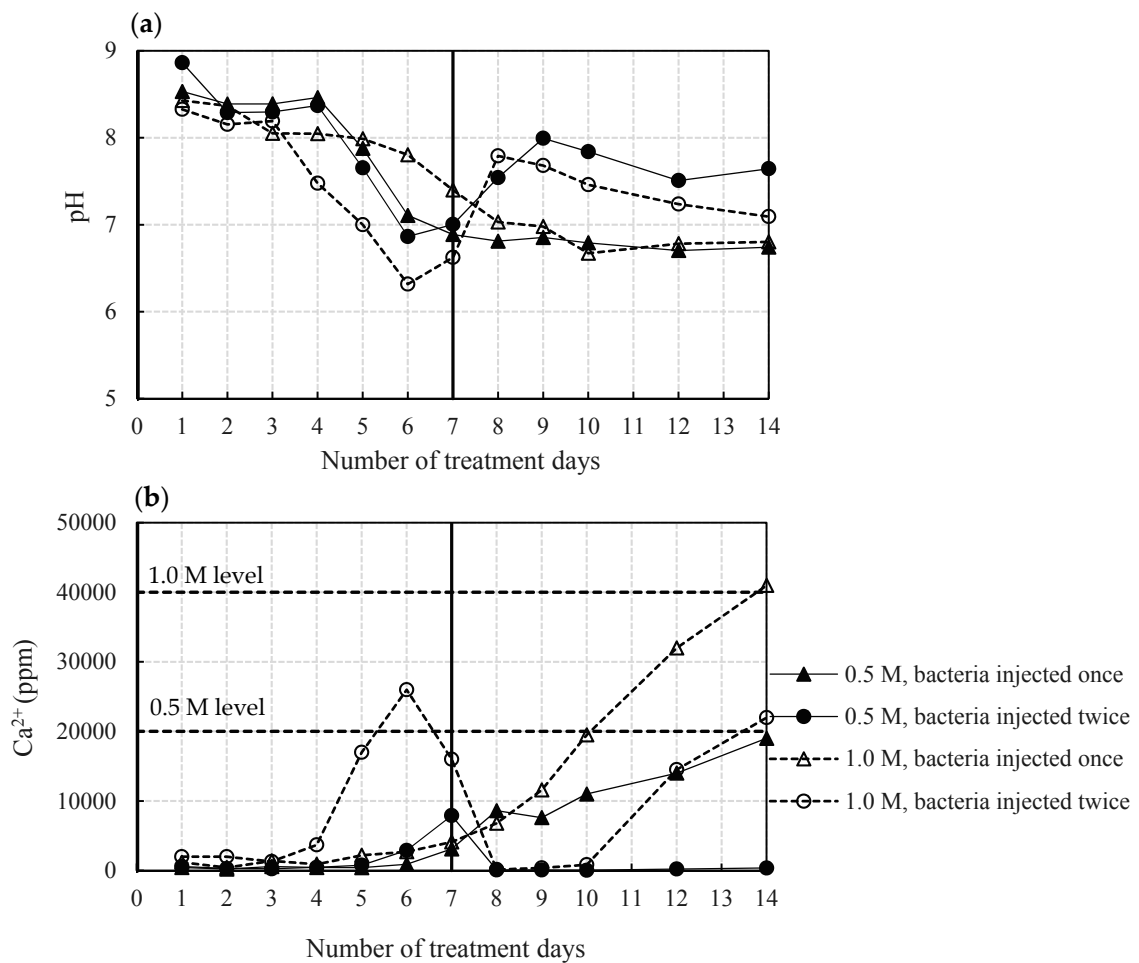


Figure 8. (a) pH; (b) Ca²⁺ measurements of the solution collected from the bottom of the sand.

In contrary to that, samples treated with 1.0 M cementation solution showed a noteworthy heterogeneity in strength distribution over the length of the column as well as among the two duplicated samples. The top portion of the specimens gained strengths as similar to or remarkably higher than their 0.5 M equivalent. However, middle and bottom portions did not harden as much as the top, and all specimens supplied with 1.0 M solution had a greater tendency to clog. The strength variation vertically along the column is suspected to happen due to several reasons. One possibility is filtering and a better accumulation of bacterial cells on top and depletion of reactant concentration as they are been readily consumed for biocementation while flowing from top to bottom [50]. This filtering mechanism is more significant in this case as the virgin beach sand used here consists of a significant percentage of fines (10.5% fines smaller than 125 μm). Additionally, the precipitated calcium carbonate crystals may act as a filter and trap bacterial cells from being washed out to the lower portions [7]. The other pertinent reason is the inhibition of the activity of the aerobic bacterium as the availability of oxygen diminishes from top to bottom [58]. The combination of these phenomena is suspected to impair the efficiency of MICP far away from the injection point.

Further, the variation in strength due to the effects of input bio-chemical concentration was investigated in detail by SEM imaging. Figure 9 highlights the differences in the microfeatures of the crystals precipitated for 0.5 M and 1.0 M cementation solutions. Overall, for all the treatment variations, rhombohedral calcium carbonate crystals were predominantly observed under SEM which is consistent with the previous findings [27,35,41,59].

For the 0.5 M cases, the CaCO_3 crystals showed a uniform precipitation pattern where the grains were covered with similar sized crystals which were very well distributed spatially on grain surfaces over the entire length of the sample. The contact areas were also covered uniformly and for the case with two bacteria injections, contact cementing and matrix supporting in the column top was characterized with larger crystals of 20–25 μm in size (Figure 9a). This pattern gave rise to a highly favorable homogeneous strength improvement in the column making it the most suitable treatment condition. But, for the case with single bacterial culture treatment, although uniformity was still maintained, only thin layers of 2–3 μm (CaCO_3 envelopes) covering individual sand particles and slightly bridging the adjacent grains were achieved which did not provide a satisfactory strength improvement.

In the case of 1.0 M treatments, although grain surfaces were predominantly covered with uniformly sized crystals, the precipitation had become more random as more calcite formed. Larger crystals of approximately 30 μm in size were randomly distributed, filling the pore spaces in the top portion and clogging near the injection point (Figure 9d). Ng et al. [54] stated that flow would be obstructed even without any specific binding of soil particles as long as precipitated crystals are larger than the pore throat. Moreover, only thin layers of differently sized CaCO_3 crystals were present away from the injection top, thus showing greatly hindered precipitation (Figure 9f).

It is reported in literature that a change in precipitation pattern in this manner can be explained by the theory behind the competition between crystal growth and crystal nucleation [24,56]. Gandhi et al. [60] in their work unraveled that the nucleation of new crystals would face a competition with the process of crystal growth if the nucleation of new crystals is permitted over the growth of existing ones. In the case of high Ca^{2+} and urea concentrations (1.0 M in current study), the cladding on grain surfaces by crystals is a result of crystal nucleation in new sites which is the initial dominant process. As the number of injections are repeated, higher and more localized pH rise around some bacterial cells take place, resulting in supersaturation due to the presence of more urea molecules and there is a greater tendency to accumulate precipitate over the initial smaller crystals rather than forming new crystals. This process will then lead to the formation of larger crystals which fill the void spaces and subsequently retard the flow of cementation solution. This has been further proved by Somani et al. [61] who stated that the average particle size of precipitate becomes larger as the carbonate concentration becomes higher.

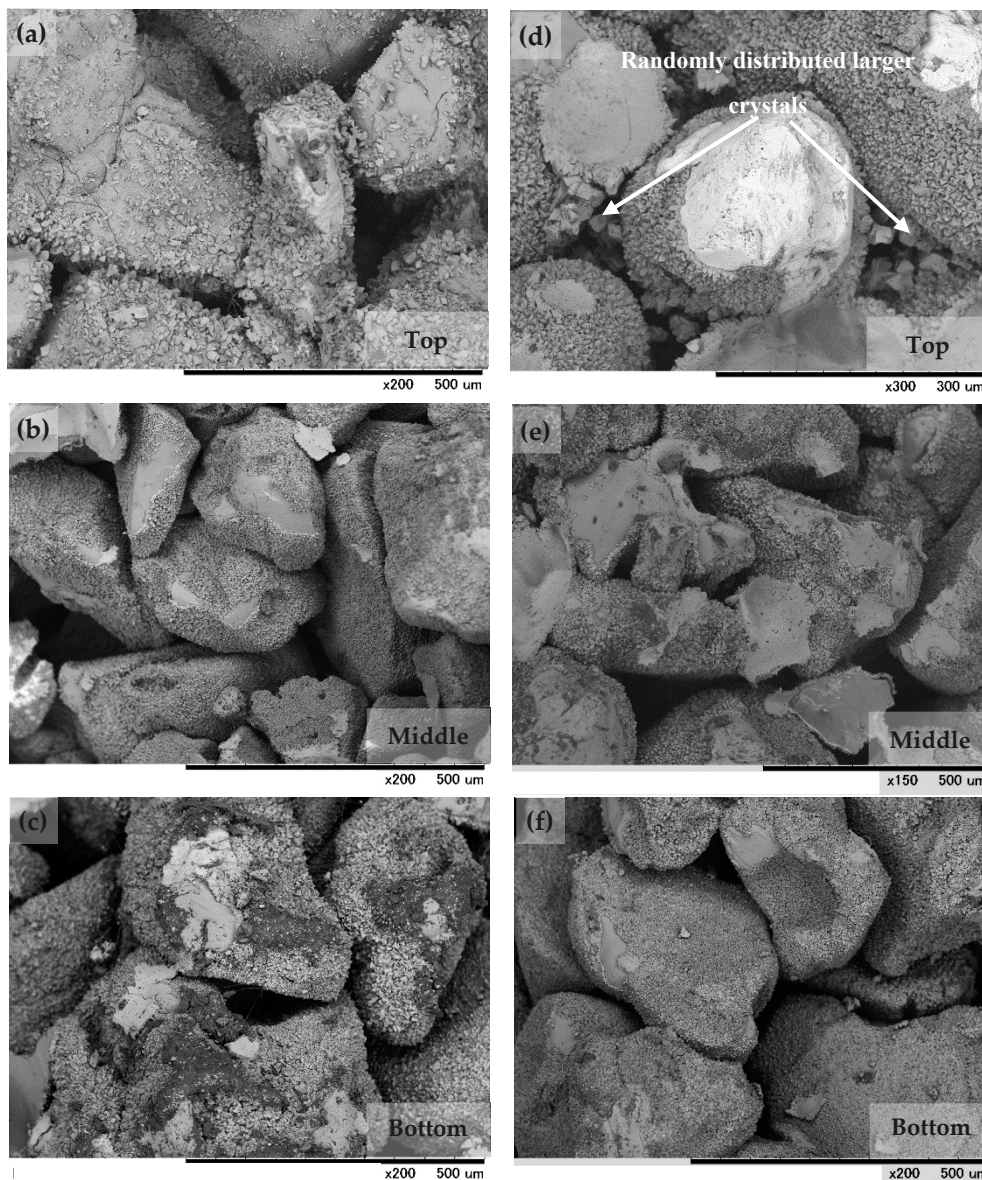


Figure 9. SEM images of showing variation of crystal morphology for the samples treated under different bacteria and reactant concentrations: (a–c) 0.5 M cementation solution with bacteria injected twice; (d–f) 1.0 M cementation solution with bacteria injected only in the beginning.

In contrast to that, the nucleation of new crystals is more dominant than the growth of existing crystals when the carbonate concentration is lower [24]. The reduced shear stresses and availability of nutrients at particle contact points cause bacteria to prefer smaller surface features like grain contacts [62] whereas cells will also be distributed over grain surfaces depending the surface properties of grains [63]. Therefore, in this case, numerous smaller crystals will be first formed which will eventually be developed to a dense crystal layer with the repeated injection of cementation solution. From these results, it is apparent that uniformly distributed smaller crystals precipitated on grain surfaces and gaps between sand particles provide better strength and homogeneity rather than continuous heterogeneous precipitation of larger crystals. This is in line with the previous findings reported in literature. Okwadha and Li [41] stated that concentrations above 0.5 M of urea and CaCl_2 reduce the efficiency of MICP. Al Qabany et al. [56] and Ng et al. [12] also demonstrated that low concentrations of cementation solution yields higher specimen strengths. Moreover, the flow rate of solutions through the column also has a crucial effect on the precipitation process and thus should be

maintained at a suitable rate for homogeneous strength improvement [64]. On the other hand, utilizing a different kind of bacteria or a different bacterial cell concentration would result in a precipitation pattern and crystal morphology different to what has been obtained in this study.

3.3.2. Effect of Mg^{2+} Addition on Microbial Induced Carbonate Precipitation

Not much investigation have been carried out so far to investigate the effect of magnesium on the microbial inspired carbonate precipitation. Nevertheless, magnesium carbonate possesses similar cementing ability as calcium carbonate, which can significantly affect the desired outcomes of MICP treatment. Figure 10 illustrates the results of MICP test tube tests incorporating Mg^{2+} .

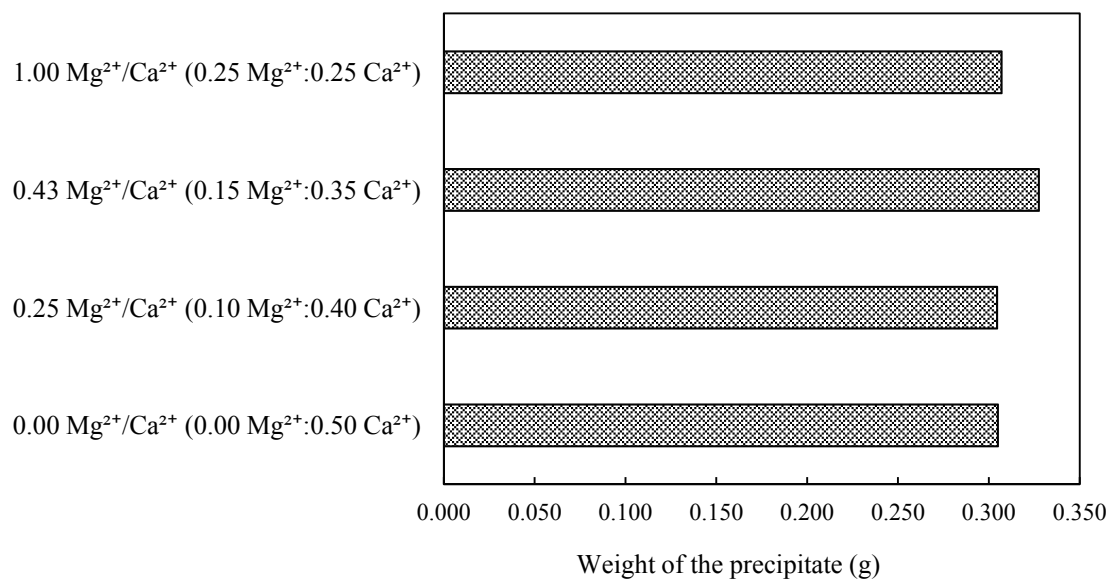


Figure 10. Variation of microbial induced carbonate precipitation under different Mg^{2+}/Ca^{2+} molar ratios.

Although Mg^{2+}/Ca^{2+} molar ratio was raised from 0 to 1, no remarkable change in the amount of precipitate was observed. However, the amount of carbonate precipitate slightly increased up to 0.43 Mg^{2+}/Ca^{2+} ratio and then decreased as Mg^{2+} was further raised until ratio became 1. Therefore, it was deduced that a Mg^{2+}/Ca^{2+} ratio approximately equaled to 0.5 is the optimum condition in this case. Similarly, in a study by Sun et al. [38] demonstrated that magnesium carbonate has a lower productive rate than calcium carbonate resulting much lower magnesium carbonate precipitation than that of calcium carbonate in any specific condition. Further, Fukue et al. [65] claimed that the total amount of precipitation decreases with an increase in Mg^{2+}/Ca^{2+} ratio from 0 to 2.3. This may be attributed to the higher solubility of magnesium carbonate which is almost one order of magnitude higher than its calcium counterpart and/or the possibility of partial hydrolysis of magnesium carbonate to generate magnesium hydroxide [38].

The size and morphology of the precipitated crystals has serious implications on the success of MICP treatment. Therefore, the microstructure and mineralogy of the precipitates from the aforementioned experimental cases were determined.

In the absence of Mg^{2+} , SEM imagery showed that the precipitate was mainly composed of entirely spherical crystals, some as large as 30–45 μm in diameter and agglomerations of relatively smaller crystals (Figure 11a). The XRD spectra revealed that the mineralogical composition was exclusively vaterite (Figure 12a), which is a metastable polymorph of $CaCO_3$. It is unstable, rapidly transforms into calcite (or aragonite) in aqueous solutions under room temperature, and forms necessarily in the presence of high supersaturation conditions [66]. The urea hydrolysis and resultant local alkalinity rise along with bacterial cells acting as nucleation sites might have developed a high supersaturation

in the medium, giving rise to massive vaterite crystallization here. On the other hand, extracellular polymeric substances (EPS) play an important role in polymorph selection [67] and vaterite crystals have been abundantly reported with a high amount of accumulated EPS [68], which is possible in this case too. Moreover, vaterite generation is also preferred with the introduction of various organic matter to the aqueous system [69].

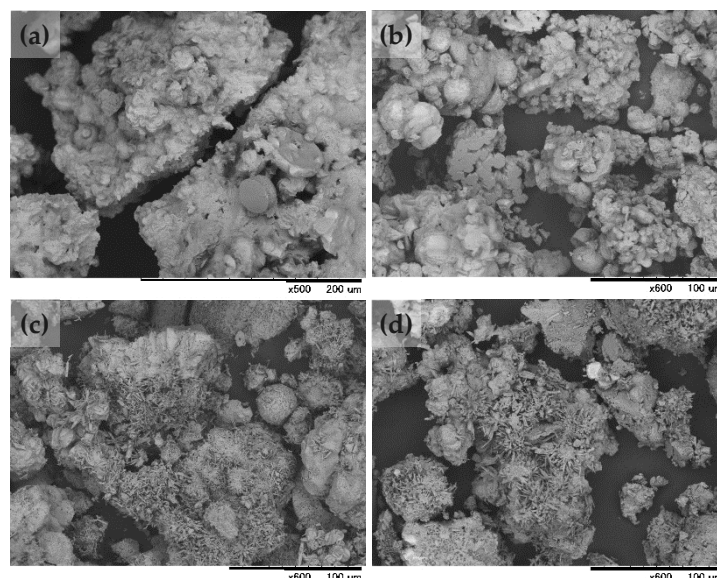


Figure 11. Scanning electron microscopy (SEM) images of microbial induced precipitate by *Sporosarcina* sp. with (a) $Mg^{2+}/Ca^{2+} = 0.00$; (b) $Mg^{2+}/Ca^{2+} = 0.25$; (c) $Mg^{2+}/Ca^{2+} = 0.43$; (d) $Mg^{2+}/Ca^{2+} = 1.00$.

As the Mg^{2+}/Ca^{2+} molar ratio was stepped up to 0.25, the calcite (and magnesium calcite) peaks emerged at the expense of the proportion of vaterite peaks (Figure 12b). The corresponding change in SEM images was the smaller spherical crystals bursting and becoming fibrous (Figure 11b), as reported by Fukue et al. [65]. When the Mg^{2+}/Ca^{2+} ratio is 0.43, aragonite was also spotted in the XRD spectra (Figure 12c). This is in consistent with the SEM images where the emergence of needle shaped crystals can be clearly seen (Figure 11c). Magnesium inducing the formation of needle/thorn shaped aragonite rather than calcite and vaterite in this manner, either abiotically or biotically, is a very well documented phenomenon in the literature [70–74]. The change of the crystals from spherical to a needle-like shape is a result of the inhibition of crystal growth in the a and b axes while allowing the same along the c axis in the presence of magnesium [65]. Substitution of Mg^{2+} until the Mg^{2+}/Ca^{2+} ratio became 1.0 increased the intensity of aragonite peaks further showing a mixture of other peaks, including calcite and magnesium calcite (Figure 12d). Subsequently, vaterite peaks disappeared. The corresponding change in the SEM micrographs is the substantial appearance of the needle shaped crystals fanning out into the space in all directions (Figure 11d).

These observations clearly revealed that although increments of Mg^{2+} did not affect the quantity of bio-induced precipitation to a great deal, the morphology of the crystals was far more sensitive to them.

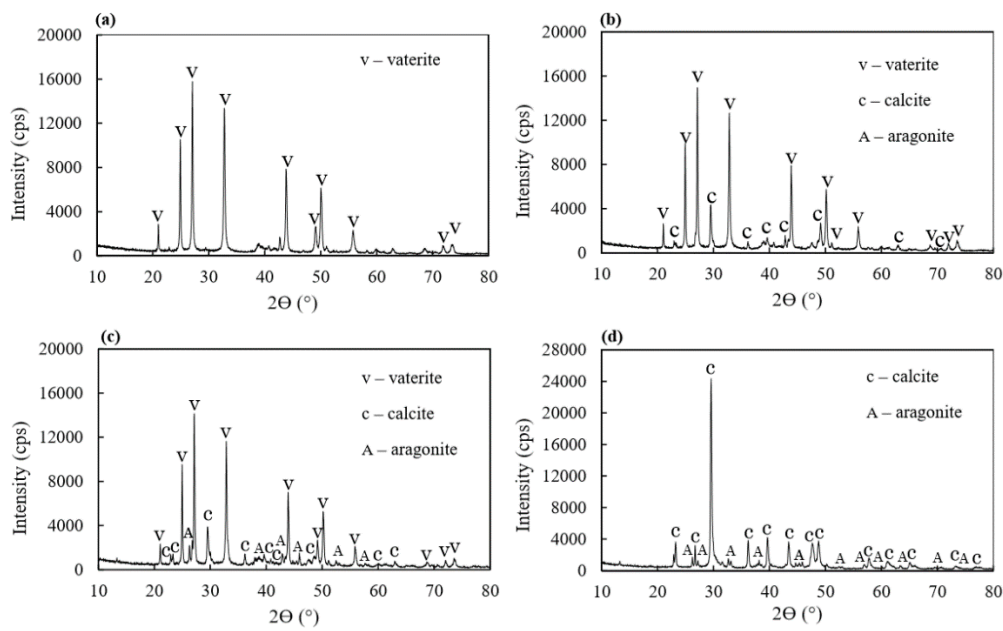


Figure 12. X-ray diffraction (XRD) spectra of the microbial induced precipitate by *Sporosarcina* sp. with (a) $Mg^{2+}/Ca^{2+} = 0.00$; (b) $Mg^{2+}/Ca^{2+} = 0.25$; (c) $Mg^{2+}/Ca^{2+} = 0.43$; (d) $Mg^{2+}/Ca^{2+} = 1.00$.

The precipitation results alone are not adequate to predict the effectiveness of MICP for beach sand solidification in the presence of magnesium. Therefore, syringe sand solidification tests were conducted and estimated UCS are displayed in Figure 13.

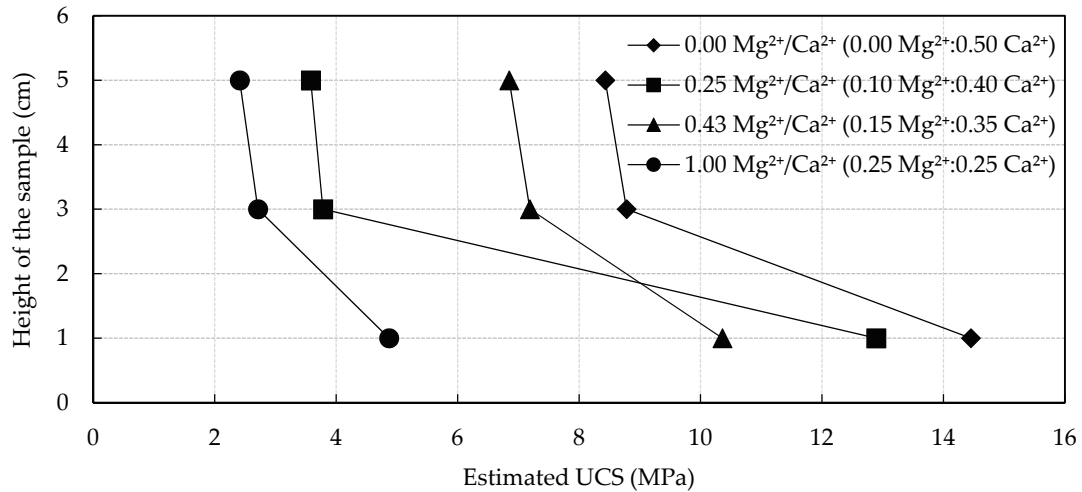


Figure 13. Variation of local strength of MICP treated sand for different Mg^{2+}/Ca^{2+} molar ratios.

Overall, it can be seen that the strength improvement by MICP treatment is considerably impaired in the presence of magnesium, and specimens without Mg^{2+} show the highest strength gain. Evidently, the specimens treated with an Mg^{2+}/Ca^{2+} ratio of 0.43 exhibit better strength than those with an Mg^{2+}/Ca^{2+} ratio of 0.25. This can be partly supported by the results of precipitation tests where the highest amount of precipitate was obtained for the $Mg^{2+}/Ca^{2+} = 0.43$ condition.

SEM microscopic observations were conducted in order to ascertain the effect of crystal morphology on strength enhancement. It is clear that the precipitated crystal morphology changed from rhombohedral to spherical and then to needle shape when the Mg^{2+}/Ca^{2+} ratio gradually advanced from 0 to 1 (Figure 14). In the absence of Mg^{2+} , the crystal morphology was exclusively rhombohedral, the typical crystalline form of calcite (Figure 14a). The grain surfaces were fully covered with crystals

of average size 10 μm and matrix was supported by relatively larger crystals (Figure 14b). The crystals were very well interweaved and crosslinked at the grain contact points thereby effectively bonding the loose sand particles together. When $\text{Mg}^{2+}/\text{Ca}^{2+}$ ratio was 0.25 only, the crystals showed slight alterations from rhombohedral form whereas contact cementing and matrix supporting seemed not as significant as in previous case (Figure 14c). As $\text{Mg}^{2+}/\text{Ca}^{2+}$ ratio was increased further to 0.43, crystals became spherical and accumulated well together at contact points (Figure 14d). Fibrous needle shaped crystals bundled together were also abundantly seen on grain surfaces as well as on contact cements. This pattern of crystal morphology resulted in a stronger bond between grains thus yielding compressive strengths closer to that without Mg^{2+} .

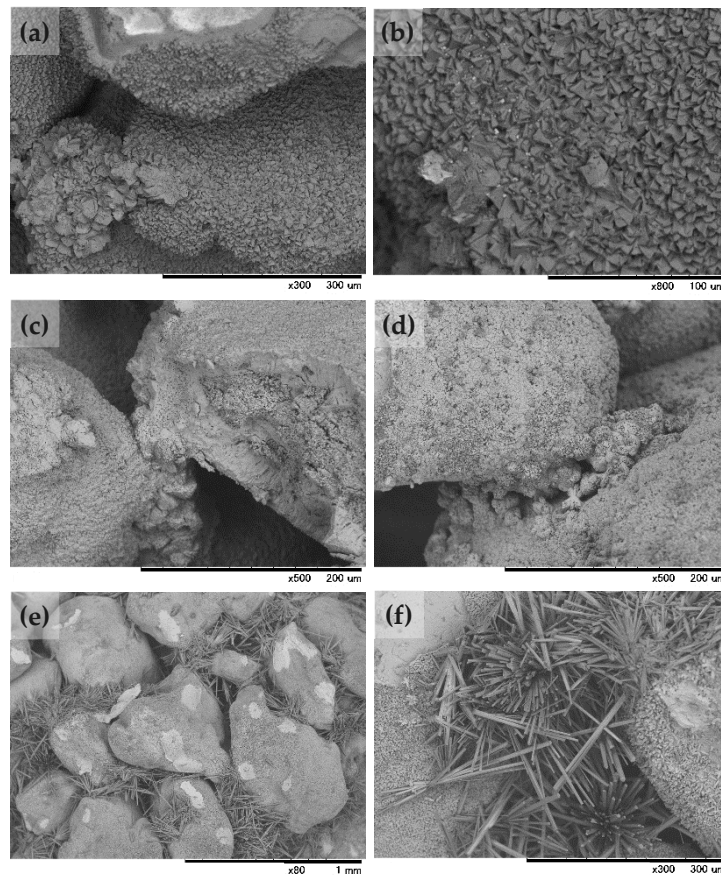


Figure 14. SEM images of variation in crystal morphology with different $\text{Mg}^{2+}/\text{Ca}^{2+}$ molar ratios: (a,b) $\text{Mg}^{2+}/\text{Ca}^{2+} = 0.00$ and its closer view; (c) $\text{Mg}^{2+}/\text{Ca}^{2+} = 0.25$; (d) $\text{Mg}^{2+}/\text{Ca}^{2+} = 0.43$; (e,f); $\text{Mg}^{2+}/\text{Ca}^{2+} = 1.00$ and its closer view.

Stepping up the $\text{Mg}^{2+}/\text{Ca}^{2+}$ ratio from 0.43 to 1.00 drastically changed the crystal morphology of the biocement. Grains were slightly cladded by small crystals while pore spaces were completely occupied by needle shaped crystals, some as long as 100–200 μm (Figure 14e,f). Apparently, these thin crystals, individually fanning out in all directions over the void spaces, had a very low binding capacity compared to the rhombohedral/spherical crystals accumulated together at grain contacts. Further, thin needle shaped crystals can be easily subjected to destruction on application of compressive forces compared to the rhombohedral or spherical crystal aggregates. These results are in good agreement with that of Gawwad et al. [73] who showed that the occurrence of needle cement in the presence of higher concentrations of magnesium deteriorates the compressive strength of the bio-mortar prepared by the common ureolytic bacterium *Sporosarcina pasteurii*. However, the majority of the studies done to address this aspect has revealed that magnesium addition enables the biocement to have a higher strength, lower porosity, and better resistance to acids compared to control samples in absence of

magnesium [19,38,65,70,75,76]. The general understanding from the above studies is that the inherent properties of aragonite, such as higher specific gravity and Mohs hardness than those of calcite and morphology which provides a denser, compact arrangement, can be the possible reason for better results. The exact reasoning to this discrepancy in results are not fully discovered yet and need more investigation.

Another interesting observation that should be noted here is the local strength variation along the sand column. Unlike the results presented under the Section 3.3.1, the estimated compressive strength increases with sand column depth. This can be attributed to the differences in particle size gradation of the two sands (sand 1 and sand 2) used. "Sand 1" is a well graded sand with a considerable amount of fines percentage while "sand 2" is a comparatively coarser uniformly graded sand. As the sand becomes finer and well graded, the sand becomes densely packed, void spaces become narrower and fewer, and the sand offers more particle-to-particle contact. The movement of bacteria through the sand column is obviously through the pore throats between grains either by self-propelled movement or by passive diffusion, and the geometric compatibility between the size of bacteria and that of the pore throat is a crucial factor [12]. In a dense particle arrangement like in sand 1, bacteria may be filtered out and cell concentration may reduce from top to bottom, whereas in a loose particle arrangement like in sand 2, bacteria may be easily flushed out with daily dose of cementation solution and retained at the bottom [44,50]. This can lead to a better cementation on top in sand 1 and on bottom for sand 2. This dictates that distribution of bacteria is a critical factor in the process.

Many researchers that have attempted to exploit the effect of grain size and gradation have presented similar results [58,77–79]. However, Dhimi et al. [58] stated that availability of oxygen plays the governing role rather than particle size distribution, thus efficacy of MICP is reduced with depth irrespective of the grain sizes. The pertinent reason for contrasting results may be that the *Sporosarcina* sp. strain used in this study has a greater tolerance to oxygen depletion than the *Bacillus megaterium* strain used in the aforementioned study, as the column length is only in centimeter scale.

4. Conclusions and Implications for the Target Application

This paper intends to report the results of a preliminary study carried out to investigate the potential of implementing microbial induced carbonate precipitation (MICP) as a novel approach towards stabilizing loose beach sand in Sri Lanka to minimize coastal erosion. This is the first study to address this aspect in the aforementioned region. After conducting a series of laboratory tests, the following conclusions were drawn.

Although ureolytic bacteria are ubiquitous in nature, not all have the required potential for MICP applications. The isolated native bacterium belonging to *Sporosarcina* sp. showed sufficient feasibility for the intended application. It is a moderately alkalo-tolerant bacterium, showing maximum growth and urease activity at an ambient temperature of 25 °C which is compatible with the tropical climate prevailing in the target region.

Laboratory scale (syringe) sand solidification test results depicted that a batch treatment of bacterial culture injected twice (in the beginning and after 7 days) with a daily injection of 0.5 M cementation solution yielded sufficiently homogeneous strength improvement after a treatment period of 14 days under saturated conditions. The residual Ca^{2+} and pH measurements of the effluent draining out from the bottom provided substantial information about the rate of urea hydrolysis and eventual calcium carbonate precipitation and can be used as good indication of the state of MICP.

Local strength analysis of two types of natural beach sand solidified by MICP exhibited that particle size and gradation, bacterial cell concentration, and the concentration of reactants have a great deal of importance on the degree and homogeneity of the strength enhancement. A precipitation pattern of uniformly distributed crystals cladding grain surfaces along with agglomerated crystal clusters at the particle contact points showed high efficiency in improving the compressive strength of biocemented sands than randomly distributed larger crystals which may result under high reactant concentrations.

Introducing magnesium into the MICP process deemed to negatively affect the desired engineering properties of the treated specimens. At the extreme, excessively high concentrations of magnesium where the Mg^{2+}/Ca^2 molar ratio was 1.0, resulted in a significant reduction in the UCS. It is clearly deduced that the strength decline is mainly due to the change in crystal morphology (rather than the quantity of precipitate) to a needle shaped crystal form with lower bonding capacity than that of the well-interweaved and cross-linked rhombohedral crystals produced in the absence of magnesium. However, the effect will be negligible in the target environment where naturally available Mg^{2+} is considerably lower compared to the concentration of Ca^{2+} supplied with the cementation solution.

On the other hand, the sand columns in this study were cemented under one-dimensional vertical flow of solutions where opted pathway of solutions were confined by syringe walls. In a real field application, the flow will be three-dimensional where flow dynamics will be dependent on numerous factors including the characteristics of the solution, sand matrix and the groundwater level.

Finally, there is still need for further experiments, under laboratory and natural conditions, in order to scale up the process and bring them to practical use. The ultimate goal of this part of the current research study was to evaluate the initial feasibility for MICP as an ecofriendly alternative approach towards beach sand stabilization and to determine the preliminary optimum conditions, making this technique one step closer to in-situ application.

Supplementary Materials: The following are available online at <http://www.mdpi.com/2076-3417/9/15/3201/s1>, Figure S1: Location map and study area, Figure S2: Particle size distribution of natural beach sand, Figure S3: Experimental set up for the syringe sand solidification test, Figure S4: Bacterial cell concentration of isolated strains.

Author Contributions: P.G.N.N. performed laboratory experiments, analysis, interpretation of data and original draft preparation; A.B.N.D. and K.N. provided technical assistance and reviewed and edited the manuscript; S.K. did primary supervision and helped in analyzing, methodical guidance, critical reviewing and approval of final version to be submitted.

Funding: This research was partially funded by JSPS KAKENHI, grant numbers JP16H04404 and JP19H02229, Japan. The authors gratefully acknowledge the support.

Conflicts of Interest: The authors declare no conflict of interest.

References

- DeJong, J.T.; Mortensen, B.M.; Martinez, B.C.; Nelson, D.C. Bio-mediated soil improvement. *Ecol. Eng.* **2010**, *36*, 197–210. [[CrossRef](#)]
- Khan, M.N.H.; Shimazaki, S.; Kawasaki, S. Coral Sand Solidification Test Through Microbial Calcium Carbonate Precipitation Using *Pararhodobacter* sp. *Int. J. GEOMATE* **2016**, *11*, 2665–2670.
- Gowthaman, S.; Mitsuyama, S.; Nakashima, K.; Komatsu, M.; Kawasaki, S. Microbial Induced Slope Surface Stabilization Using Industrial-Grade Chemicals: A Preliminary Laboratory Study. *Int. J. GEOMATE* **2019**, *17*, 110–116. [[CrossRef](#)]
- Van Paassen, L.A.; Ghose, R.; van der Linden, T.J.M.; van der Star, W.R.L.; van Loosdrecht, M.C.M. Quantifying Biomediated Ground Improvement by Ureolysis: Large-Scale Biogrout Experiment. *J. Geotech. Geoenviron. Eng.* **2010**, *136*, 1721–1728. [[CrossRef](#)]
- Gomez, M.G.; Anderson, C.M.; Graddy, C.M.R.; DeJong, J.T.; Nelson, D.C.; Ginn, T.R. Large-Scale Comparison of Bioaugmentation and Biostimulation Approaches for Biocementation of Sands. *J. Geotech. Geoenviron. Eng.* **2016**, *143*, 04016124. [[CrossRef](#)]
- Canakci, H.; Sidik, W.; Halil Kilic, I. Effect of bacterial calcium carbonate precipitation on compressibility and shear strength of organic soil. *Soils Found.* **2015**, *55*, 1211–1221. [[CrossRef](#)]
- Cheng, L.; Cord-Ruwisch, R. In situ soil cementation with ureolytic bacteria by surface percolation. *Ecol. Eng.* **2012**, *42*, 64–72. [[CrossRef](#)]
- Zhao, Y.; Yao, J.; Yuan, Z.; Wang, T.; Zhang, Y.; Wang, F. Bioremediation of Cd by strain GZ-22 isolated from mine soil based on biosorption and microbially induced carbonate precipitation. *Environ. Sci. Pollut. Res.* **2017**, *24*, 372–380. [[CrossRef](#)]
- Wu, J.; Wang, X.B.; Wang, H.F.; Zeng, R.J. Microbially induced calcium carbonate precipitation driven by ureolysis to enhance oil recovery. *RSC Adv.* **2017**, *7*, 37382–37391. [[CrossRef](#)]

10. Okyay, T.O.; Nguyen, H.N.; Castro, S.L.; Rodrigues, D.F. CO₂ sequestration by ureolytic microbial consortia through microbially-induced calcite precipitation. *Sci. Total Environ.* **2016**, *572*, 671–680. [[CrossRef](#)]
11. Mwandira, W.; Nakashima, K.; Kawasaki, S.; Ito, M.; Sato, T.; Igarashi, T.; Banda, K.; Chirwa, M.; Nyambe, I.; Nakayama, S.; et al. Efficacy of biocementation of lead mine waste from the Kabwe Mine site evaluated using *Pararhodobacter* sp. *Environ. Sci. Pollut. Res.* **2019**, *26*, 15653–15664. [[CrossRef](#)] [[PubMed](#)]
12. Ng, W.S.; Lee, M.-L.; Hii, S.-L. An Overview of the Factors Affecting Microbial-Induced Calcite Precipitation and its Potential Application in Soil Improvement. *Int. J. Civ. Environ. Eng.* **2012**, *6*, 188–194.
13. Stocks-Fischer, S.; Galinat, J.K.; Bang, S.S. Microbiological precipitation of CaCO₃. *Soil Biol. Biochem.* **1999**, *31*, 1563–1571. [[CrossRef](#)]
14. Harkes, M.P.; van Paassen, L.A.; Booster, J.L.; Whiffin, V.S.; van Loosdrecht, M.C.M. Fixation and distribution of bacterial activity in sand to induce carbonate precipitation for ground reinforcement. *Ecol. Eng.* **2010**, *36*, 112–117. [[CrossRef](#)]
15. Cortés, P.; Escrig, C.; Bernat-Maso, E.; Gil, L.; Barbé, J. Effect of *Sporosarcina pasteurii* on the strength properties of compressed earth specimens. *Mater. Construcción* **2018**, *68*, 143.
16. Whiffin, V.S.; van Paassen, L.A.; Harkes, M.P. Microbial carbonate precipitation as a soil improvement technique. *Geomicrobiol. J.* **2007**, *24*, 417–423. [[CrossRef](#)]
17. Temmerman, S.; Meire, P.; Bouma, T.J.; Herman, P.M.J.; Ysebaert, T.; De Vriend, H.J. Ecosystem-based coastal defence in the face of global change. *Nature* **2013**, *504*, 79–83. [[CrossRef](#)]
18. Ten Voorde, M.; do Carmo, J.S.A.; Neves, M.G. Designing a Preliminary Multifunctional Artificial Reef to Protect the Portuguese Coast. *J. Coast. Res.* **2009**, *251*, 69–79. [[CrossRef](#)]
19. Cheng, L.; Shahin, M.A.; Cord-Ruwisch, R. Bio-cementation of sandy soil using microbially induced carbonate precipitation for marine environments. *Géotechnique* **2014**, *64*, 1010–1013. [[CrossRef](#)]
20. Salifu, E.; MacLachlan, E.; Iyer, K.R.; Knapp, C.W.; Tarantino, A. Application of microbially induced calcite precipitation in erosion mitigation and stabilisation of sandy soil foreshore slopes: A preliminary investigation. *Eng. Geol.* **2016**, *201*, 96–105. [[CrossRef](#)]
21. Chu, J.; Ivanov, V.; Chenghong, G.; Naeimi, M.; Tkalic, P. Microbial geotechnical engineering for disaster mitigation and coastal management. *Proc. Earthq. Tsunami* **2009**, 1–6.
22. Shanahan, C.; Montoya, B.M. *Strengthening Coastal Sand Dunes Using Microbial-Induced Calcite Precipitation*; Geo-Congress 2014 Technical Papers; American Society of Civil Engineers (ASCE): Reston, VA, USA, 2014; pp. 1683–1692.
23. Van der Ruyt, M.; van der Zon, W. Biological in situ reinforcement of sand in near-shore areas. *Proc. Inst. Civ. Eng. Geotech. Eng.* **2009**, *162*, 81–83. [[CrossRef](#)]
24. Cheng, L.; Shahin, M.A.; Mujah, D. Influence of Key Environmental Conditions on Microbially Induced Cementation for Soil Stabilization. *J. Geotech. Geoenviron. Eng.* **2016**, *143*, 04016083-1–04016083-11. [[CrossRef](#)]
25. Gat, D.; Tsesarsky, M.; Shamir, D.; Ronen, Z. Accelerated microbial-induced CaCO₃ precipitation in a defined coculture of ureolytic and non-ureolytic bacteria. *Biogeosciences* **2014**, *11*, 2561–2569. [[CrossRef](#)]
26. De Muynck, W.; De Belie, N.; Verstraete, W. Microbial carbonate precipitation in construction materials: A review. *Ecol. Eng.* **2010**, *36*, 118–136. [[CrossRef](#)]
27. Lin, H.; Suleiman, M.T.; Brown, D.G.; Kavazanjian, E. Mechanical Behavior of Sands Treated by Microbially Induced Carbonate Precipitation. *J. Geotech. Geoenviron. Eng.* **2015**, *142*, 04015066. [[CrossRef](#)]
28. Gat, D.; Ronen, Z.; Tsesarsky, M. Soil Bacteria Population Dynamics Following Stimulation for Ureolytic Microbial-Induced CaCO₃ Precipitation. *Environ. Sci. Technol.* **2016**, *50*, 616–624. [[CrossRef](#)] [[PubMed](#)]
29. Tobler, D.J.; Cuthbert, M.O.; Greswell, R.B.; Riley, M.S.; Renshaw, J.C.; Handley-Sidhu, S.; Phoenix, V.R. Comparison of rates of ureolysis between *Sporosarcina pasteurii* and an indigenous groundwater community under conditions required to precipitate large volumes of calcite. *Geochim. Cosmochim. Acta* **2011**, *75*, 3290–3301. [[CrossRef](#)]
30. Dhami, N.K.; Alsubhi, W.R.; Watkin, E.; Mukherjee, A. Bacterial community dynamics and biocement formation during stimulation and augmentation: Implications for soil consolidation. *Front. Microbiol.* **2017**, *8*, 1267. [[CrossRef](#)]
31. Wenderoth, D.F.; Rosenbrock, P.; Abraham, W.R.; Pieper, D.H.; Höfle, M.G. Bacterial community dynamics during biostimulation and bioaugmentation experiments aiming at chlorobenzene degradation in groundwater. *Microb. Ecol.* **2003**, *46*, 161–176. [[CrossRef](#)]

32. Nawarathna, T.H.K.; Nakashima, K.; Fujita, M.; Takatsu, M.; Kawasaki, S. Effects of Cationic Polypeptide on CaCO₃ Crystallization and Sand Solidification by Microbial-Induced Carbonate Precipitation. *ACS Sustain. Chem. Eng.* **2018**, *6*, 10315–10322. [[CrossRef](#)]
33. Graddy, C.M.R.; Gomez, M.G.; Kline, L.M.; Morrill, S.R.; Dejong, J.T.; Nelson, D.C. Diversity of *Sporosarcina*-like Bacterial Strains Obtained from Meter-Scale Augmented and Stimulated Biocementation Experiments. *Environ. Sci. Technol.* **2018**, *52*, 3997–4005. [[CrossRef](#)] [[PubMed](#)]
34. Sun, Y.; Zhao, Q.; Zhi, D.; Wang, Z.; Wang, Y.; Xie, Q.; Wu, Z.; Wang, X.; Li, Y.; Yu, L.; et al. *Sporosarcina terrae* sp. Nov., isolated from orchard soil. *Int. J. Syst. Evol. Microbiol.* **2017**, *67*, 2104–2108. [[CrossRef](#)] [[PubMed](#)]
35. Dick, J.; De Windt, W.; De Graef, B.; Saveyn, H.; Van Der Meeren, P.; De Belie, N.; Verstraete, W. Bio-deposition of a calcium carbonate layer on degraded limestone by *Bacillus* species. *Biodegradation* **2006**, *17*, 357–367. [[CrossRef](#)] [[PubMed](#)]
36. Achal, V.; Mukherjee, A.; Basu, P.C.; Reddy, M.S. Strain improvement of *Sporosarcina pasteurii* for enhanced urease and calcite production. *J. Ind. Microbiol. Biotechnol.* **2009**, *36*, 981–988. [[CrossRef](#)] [[PubMed](#)]
37. Hammad, I.A.; Talkhan, F.N.; Zoheir, A.E. Urease activity and induction of calcium carbonate precipitation by *Sporosarcina pasteurii* NCIMB 8841. *J. Appl. Sci. Res.* **2013**, *9*, 1525–1533.
38. Sun, X.; Miao, L.; Wu, L.; Wang, C. Study of magnesium precipitation based on biocementation. *Mar. Georesour. Geotechnol.* **2019**. [[CrossRef](#)]
39. Kang, C.H.; Choi, J.H.; Noh, J.G.; Kwak, D.Y.; Han, S.H.; So, J.S. Microbially Induced Calcite Precipitation-based Sequestration of Strontium by *Sporosarcina pasteurii* WJ-2. *Appl. Biochem. Biotechnol.* **2014**, *174*, 2482–2491. [[CrossRef](#)] [[PubMed](#)]
40. Bang, S.S.; Galinat, J.K.; Ramakrishnan, V. Calcite precipitation induced by polyurethane-immobilized *Bacillus pasteurii*. *Enzyme Microb. Technol.* **2001**, *28*, 404–409. [[CrossRef](#)]
41. Okwadha, G.D.O.; Li, J. Optimum conditions for microbial carbonate precipitation. *Chemosphere* **2010**, *81*, 1143–1148. [[CrossRef](#)]
42. Fujita, Y.; Grant Ferris, F.; Daniel Lawson, R.; Colwell, F.S.; Smith, R.W. Calcium carbonate precipitation by ureolytic subsurface bacteria. *Geomicrobiol. J.* **2000**, *17*, 305–318. [[CrossRef](#)]
43. Anbu, P.; Kang, C.H.; Shin, Y.J.; So, J.S. Formations of calcium carbonate minerals by bacteria and its multiple applications. *Springerplus* **2016**, *5*, 1–26. [[CrossRef](#)] [[PubMed](#)]
44. Rebata-Landa, V. Microbial Activity in Sediments: Effects on Soil Behavior. Ph.D. Thesis, Georgia Institute of Technology, Atlanta, GA, USA, 2007.
45. Dhami, N.K.; Reddy, M.S.; Mukherjee, A. Synergistic role of bacterial urease and carbonic anhydrase in carbonate mineralization. *Appl. Biochem. Biotechnol.* **2014**, *172*, 2552–2561. [[CrossRef](#)] [[PubMed](#)]
46. Sahrawat, K.L. Effects of temperature and moisture on urease activity in semi-arid tropical soils. *Plant Soil* **1984**, *8*, 401–408. [[CrossRef](#)]
47. Liang, Z.P.; Feng, Y.Q.; Meng, S.X.; Liang, Z.Y. Preparation and properties of urease immobilized onto Glutaraldehyde cross-linked Chitosan beads. *Chin. Chem. Lett.* **2005**, *16*, 135–138.
48. Chen, Y.Y.M.; Anne Clancy, K.; Burne, R.A. *Streptococcus salivarius* urease: Genetic and biochemical characterization and expression in a dental plaque streptococcus. *Infect. Immun.* **1996**, *64*, 585–592.
49. Fujita, M.; Nakashima, K.; Achal, V.; Kawasaki, S. Whole-cell evaluation of urease activity of *Pararhodobacter* sp. isolated from peripheral beachrock. *Biochem. Eng. J.* **2017**, *124*, 1–5. [[CrossRef](#)]
50. Van Paassen, L.A. Biogrout: Ground Improvement by Microbially Induced Carbonate Precipitation. Ph.D. Thesis, Delft University of Technology, Delft, The Netherlands, 2009.
51. Mobley, H.L.T.; Island, M.D.; Hausinger, R.P. Molecular biology of microbial ureases. *Microbiol. Rev.* **1995**, *59*, 451–480. [[PubMed](#)]
52. Ciurli, S.; Marzadori, C.; Benini, S.; Deiana, S.; Gessa, C. Urease from the soil bacterium *Bacillus pasteurii*: Immobilization on Ca- polygalacturonate. *Soil Biol. Biochem.* **1996**, *28*, 811–817. [[CrossRef](#)]
53. Mahadevan, S.; Sauer, F.D.; Erfle, J.D. Purification and properties of urease from bovine rumen. *Biochem. J.* **2015**, *163*, 495–501. [[CrossRef](#)]
54. Ng, W.S.; Lee, L.M.; Khun, T.C.; Ling, H.S. Factors Affecting Improvement in Engineering Properties of Residual Soil through Microbial-Induced Calcite Precipitation. *J. Geotech. Geoenviron. Eng.* **2014**, *140*, 04014006.
55. Zhu, T.; Dittrich, M. Carbonate Precipitation through Microbial Activities in Natural Environment, and Their Potential in Biotechnology: A Review. *Front. Bioeng. Biotechnol.* **2016**, *4*, 1–21. [[CrossRef](#)] [[PubMed](#)]

56. Al Qabany, A.; Soga, K.; Santamarina, C. Factors Affecting Efficiency of Microbially Induced Calcite Precipitation. *J. Geotech. Geoenviron. Eng.* **2011**, *138*, 992–1001. [[CrossRef](#)]
57. Li, W.; Liu, L.P.; Zhou, P.P.; Cao, L.; Yu, L.J.; Jiang, S.Y. Calcite precipitation induced by bacteria and bacterially produced carbonic anhydrase. *Curr. Sci.* **2011**, *100*, 502–508.
58. Dhamsi, N.K.; Reddy, M.S.; Mukherjee, A. Significant indicators for biomineralisation in sand of varying grain sizes. *Constr. Build. Mater.* **2016**, *104*, 198–207. [[CrossRef](#)]
59. Gorospe, C.M.; Han, S.H.; Kim, S.G.; Park, J.Y.; Kang, C.H.; Jeong, J.H.; So, J.S. Effects of different calcium salts on calcium carbonate crystal formation by *Sporosarcina pasteurii* KCTC 3558. *Biotechnol. Bioprocess Eng.* **2013**, *18*, 903–908. [[CrossRef](#)]
60. Gandhi, K.S.; Kumar, R.; Ramkrishna, D. Some Basic Aspects of Reaction Engineering of Precipitation Processes. *Ind. Eng. Chem. Res.* **1995**, *34*, 3223–3230. [[CrossRef](#)]
61. Somani, R.S.; Patel, K.S.; Mehta, A.R.; Jasra, R.V. Examination of the polymorphs and particle size of calcium carbonate precipitated using still effluent (i.e., CaCl₂ + NaCl solution) of soda ash manufacturing process. *Ind. Eng. Chem. Res.* **2006**, *45*, 5223–5230. [[CrossRef](#)]
62. Mujah, D.; Shahin, M.A.; Cheng, L. State-of-the-Art Review of Biocementation by Microbially Induced Calcite Precipitation (MICP) for Soil Stabilization. *Geomicrobiol. J.* **2017**, *34*, 524–537. [[CrossRef](#)]
63. Chu, J.; Ivanov, V.; Naeimi, M.; Stabnikov, V.; Liu, H.L. Optimization of calcium-based bioclogging and biocementation of sand. *Acta Geotech.* **2014**, *9*, 277–285. [[CrossRef](#)]
64. Mortensen, B.M.; Haber, M.J.; DeJong, J.T.; Caslake, L.F.; Nelson, D.C. Effects of environmental factors on microbial induced calcium carbonate precipitation. *J. Appl. Microbiol.* **2011**, *111*, 338–349. [[CrossRef](#)] [[PubMed](#)]
65. Fukue, M.; Ono, S.-I.; Sato, Y. Cementation of Sands Due To Microbiologically-Induced Carbonate Precipitation. *Soils Found.* **2011**, *51*, 83–93. [[CrossRef](#)]
66. Spanos, N.; Koutsoukos, P.G. The transformation of vaterite to calcite: Effect of the conditions of the solutions in contact with the mineral phase. *J. Cryst. Growth* **1998**, *191*, 783–790. [[CrossRef](#)]
67. Bains, A.; Dhamsi, N.K.; Mukherjee, A.; Reddy, M.S. Influence of Exopolymeric Materials on Bacterially Induced Mineralization of Carbonates. *Appl. Biochem. Biotechnol.* **2015**, *175*, 3531–3541. [[CrossRef](#)] [[PubMed](#)]
68. Gowthaman, S.; Mitsuyama, S.; Nakashima, K.; Komatsu, M.; Kawasaki, S. Biogeotechnical approach for slope soil stabilization using locally isolated bacteria and inexpensive low-grade chemicals: A feasibility study on Hokkaido expressway soil, Japan. *Soils Found.* **2019**, *59*, 484–499. [[CrossRef](#)]
69. Nawarathna, T.H.K.; Nakashima, K.; Kawasaki, S. Chitosan enhances calcium carbonate precipitation and solidification mediated by bacteria. *Int. J. Biol. Macromol.* **2019**, *133*, 867–874. [[CrossRef](#)] [[PubMed](#)]
70. Putra, H.; Kinoshita, N.; Yasuhara, H.; Lu, C.-W.; Neupane, D. Effect of Magnesium as Substitute Material in Enzyme-Mediated Calcite Precipitation for Soil-Improvement Technique. *Front. Bioeng. Biotechnol.* **2016**, *4*, 37. [[CrossRef](#)] [[PubMed](#)]
71. Meiri, W.; Korchef, A.; Tlili, M.; Ben Amor, M. Effects of temperature on precipitation kinetics and microstructure of calcium carbonate in the presence of magnesium and sulphate ions. *Desalin. Water Treat.* **2014**, *52*, 4863–4870. [[CrossRef](#)]
72. Oomori, T.; Kitano, Y. The effect of Magnesium ions on the polymorphic crystallization of calcium carbonate. *Bull. Coll. Sci. Univ. Ryukyus* **1985**, *39*, 57–62.
73. Gawwad, H.A.A.; Mohamed, S.A.E.A.; Mohammed, S.A. Impact of magnesium chloride on the mechanical properties of innovative bio-mortar. *Mater. Lett.* **2016**, *178*, 39–43. [[CrossRef](#)]
74. Putra, H.; Yasuhara, H.; Kinoshita, N.; Hirata, A. Optimization of Enzyme-Mediated Calcite Precipitation as a Soil-Improvement Technique: The Effect of Aragonite and Gypsum on the Mechanical Properties of Treated Sand. *Crystals* **2017**, *7*, 59. [[CrossRef](#)]
75. Sun, X.; Miao, L. The Comparison of Microbiologically-Induced Calcium Carbonate Precipitation and Magnesium Carbonate Precipitation. In *Proceedings of the 8th International Congress on Environmental Geotechnics*; Springer Nature Singapore Pte Ltd.: Singapore, 2019; Volume 3, pp. 302–308.
76. Rong, H.; Qian, C.X.; Li, L.Z. Influence of Magnesium Additive on Mechanical Properties of Microbe Cementitious Materials. *Mater. Sci. Forum* **2013**, *743–744*, 275–279. [[CrossRef](#)]
77. Mahawish, A.; Bouazza, A.; Gates, W.P. Effect of particle size distribution on the bio-cementation of coarse aggregates. *Acta Geotech.* **2018**, *13*, 1019–1025. [[CrossRef](#)]

78. Sharma, A.; Ramkrishnan, R. Study on effect of Microbial Induced Calcite Precipitates on strength of fine grained soils. *Perspect. Sci.* **2016**, *8*, 198–202. [[CrossRef](#)]
79. Deng, W.; Wang, Y. Investigating the Factors Affecting the Properties of Coral Sand Treated with Microbially Induced Calcite Precipitation. *Adv. Civ. Eng.* **2018**, *2018*, 1–6. [[CrossRef](#)]



© 2019 by the authors. Licensee MDPI, Basel, Switzerland. This article is an open access article distributed under the terms and conditions of the Creative Commons Attribution (CC BY) license (<http://creativecommons.org/licenses/by/4.0/>).